RSC Advances

Cite this: DOI: 10.1039/c0xx00000x

www.rsc.org/xxxxxx

ARTICLE TYPE

Facile Microwave-assisted Synthesis and Effective Photocatalytic Hydrogen Generation of Zn_2GeO_4 with different morphology

Min Yang, Ying Ji, Wei Liu, Ying Wang, Xiaoyang Liu*

Received (in XXX, XXX) Xth XXXXXXXXX 20XX, Accepted Xth XXXXXXXXX 20XX
DOI: 10.1039/b000000x

Single-crystalline hexagonal prism Zn_2GeO_4 nanorods and hierarchical Zn_2GeO_4 microspheres have been successfully synthesized via a facile microwave-assisted solution-phase approach. The as-prepared samples were characterized by XRD, SEM, TEM, HRTEM and UV-vis diffuse reflectance spectrum. The hierarchical Zn_2GeO_4 microspheres were found to be constructed of randomly aggregated nanorods which have dimensions of about 50 nm in length and 20 nm in width. Such rhombohedral phase Zn_2GeO_4 nanorods were found to be 10 – 20 nm in diameter and ~ 200 nm in length. Some influencing factors such as the reaction time, temperature, the urea were revealed to play crucial roles in the formation of Zn_2GeO_4 photocatalysts. A possible growth mechanism was proposed based on the experimental results. The rhombohedral phase Zn_2GeO_4 nanorods exhibited superior photocatalytic activities for the photocatalytic decomposition of water-methanol solution to hydrogen under UV irradiation.

Introduction

Solar-driven photocatalytic hydrogen evolution over semiconductor materials has an alluring potential for obtaining clean fuel from renewable resources[1, 2]. Zinc germanate (Zn_2GeO_4) has attracted wide attention due to its increasing application in photocatalysis and environmental remediation[3, 4]. In particular, both experimental results and theoretical analysis indicate that its electronic structure is very suitable for use as a photocatalyst[5]. Over the years, various types of Zn_2GeO_4 nanostructures including nanowires[6], nanorods[7], nanoribbons, and microspheres have been prepared by different methods and showed good activities for various kinds of photocatalytic reactions[8-11]. The universality of the photocatalytic function of Zn_2GeO_4 attracts extensive interest and attention[12]. The design and development of highly active photocatalysts has been a challenging research subject in the field.

Several solution routes and gas phase evaporation techniques have been developed for the preparation of nanorods, nanoribbons and nanowires of Zn_2GeO_4[12-14]. However, most of the reported routes were related to a complex reaction process[15, 16]. The surfactant, high-temperature and high-pressure were usually used to control the morphology of the final product, which are not beneficial for obtaining the high-purity and low defect-density product[17]. To the best of our knowledge, only several reports have appeared on the fabrication of the 1-D Zn_2GeO_4. Huang *et al*. reported the synthesis of Zn_2GeO_4 nanorods by a surfactant- assisted hydrothermal method[18]. Yan and co-workers have prepared ternary Zn_2GeO_4 nanowires and their branched structures by a chemical vapor transport method[19]. These reported procedures usually require long reaction times. A facile and fast solution-based procedure is highly desired for the preparation of Zn_2GeO_4 photocatalyst materials. In recent years, microwave heating has been widely applied in chemical reactions and materials synthesis[20, 21]. Zhu *et al*, reported MW irradiation can promote the nucleation and growth stage of nanocrystals[22]. The introduction of microwave to chemical synthesis is important in material science and engineering, and it has been proved to be a fast technology with high yields and reproducibility[23-25]. In comparison to conventional heating, the unique microwave dielectric heating mechanism can accelerate the reaction rate much more effectively[20, 26-28]. However, there were few reports about microwave-assisted synthesis of Zn_2GeO_4 photo-catalyst materials, especially micro-nano structured exhibited superior photocatalytic activities for the photocatalytic decomposition of water-methanol solution to hydrogen[29].

Herein, we report the successful synthesis of Zn_2GeO_4 nanorods and microspheres through a facile and rapid microwave-assisted solution-phase route. It is shown that the obtained samples indeed exhibit outstanding photocatalytic activities without any co-catalyst for hydrogen production from methanol–water solution. The formation process of the bundle and the correlations between morphology and photocatalytic activities were discussed.

Experimental

Preparation of hexagonal Zn_2GeO_4 nanorods. The Zn_2GeO_4 nanorods were synthesized via a facile microwave-assisted solution-phase method without any surfactant assistance. In a typical synthetic procedure, GeO_2 and $Zn(CH_3COO)_2·H_2O$ were added to 40 mL of deionized water. The mixture was stirred for 30 min. Then NaOH solution (5 mol/L) was introduced dropwise to the vigorously stirred solution to adjust pH to 8. After additional agitation for 20 min, the obtained white colloidal precipitate was transferred into a microwave glass vessel, sealed and maintained at 140 ºC for 1-10 min using a single-mode Microwave synthesizer, then cooled naturally to room temperature. The products were dried at 80 ºC for 12 h. Bulk Zn_2GeO_4 was prepared by a conventional solid-state reaction. 0.2092 g GeO_2 and 0.3256 g ZnO powders were ground and mixed thoroughly in an agate mortar. The resulting mixture was sintered at 1200 ºC (ramp rate 5 ºC/min) for 16 h in air to produce bulk Zn_2GeO_4[12, 30].

Preparation of Hierarchical Zn_2GeO_4 microspheres. 1.190 g $Zn(NO_3)_2·6H_2O$ and 3.604 g urea were firstly dissolved in 35 mL deionized water with stirring. Then, 0.209 g GeO_2 was added to the solution and the mixture was further stirred for 20 min. The as –obtained white colloidal precipitate was transferred into a microwave glass vessel, sealed and maintained at 170 ºC for 1-10 min using a single-mode Microwave synthesizer, Then cooled naturally to room temperature. After the hydrothermal reaction, the products were collected, centrifuged, washed with deionized water for five times. Finally, the white powders were obtained by drying the products at 80 ºC.

Characterization

The resultant phases of the samples were characterized by X-ray diffraction (XRD, Cu Kα radiation, Rigaku D/max2550VB, Japan). The morphology and structures of samples were observed using scanning electron microscopy (SEM, JSM-6700F, JEOL, Japan) equipped with an energy dispersive X-ray (EDX) spectrometer. The transmission electron microscopy (TEM) and high-resolution TEM (HRTEM) images were obtained on a FEI Tecnai G2S-Twin with a field emission gun operating at 200 kV. The UV/Vis diffuse reflectance spectra were recorded on a Perkin-Elmer Lambda 20 UV/Vis spectrometer. The microwave system was a single-mode Microwave Synthesizer (Biotage AB, Uppsala, Sweden)

Photocatalytic performance

The photocatalytic hydrogen evolution reaction was performed in a closed gas-recirculation system equipped with a quartz reaction vessel with inner irradiation. 0.075 g of photocatalyst was dispersed in 75 mL of H_2O by magnetic stirring. Prior to the reaction, the system was evacuated by a mechanical pump and then filled with 101 kPa high-purity N_2 (>99.99%). This process was repeated three times in order to completely remove O_2 from the system. After that, 5 mL of CH_3OH was introduced into the reactor with a syringe. The suspension was irradiated with a 125 W ultraviolet mercury lamp (GGZ-125). The temperature of the solution was controlled at room temperature by circulating water. The evolved hydrogen gas was circulated with a microdiaphragm gas pump in the system and its amount was determined by an online gas chromatograph.

Results and discussion

Hydrothermal synthesis has been extensively used to promote preferred growth nanorod, nanoflower and microspheres. However it is hard to control the size and morphology uniformity of the product due to its inhomogeneous environment during long reaction times (~10-24 hours). Single-mode microwave irradiation can offer a homogenous reaction environment, which has been suggested as an effective tool to obtain photocatalyst with uniform dispersion and size and morphology control. The microwave-assisted hydrothermal reaction time is only 10 min. Fig. 1a shows the XRD patterns of the bulk Zn_2GeO_4 (1200 ºC, 16 h) and Zn_2GeO_4 samples prepared by the microwave-assisted hydrothermal method. All the diffraction peaks of the Zn_2GeO_4 sample can be assigned to a pure rhombohedral Zn_2GeO_4 phase (JCPDS No. 11-0687). No characteristic peaks of other impurities such as ZnO and GeO_2 were observed. From the Fig. 1a, it can been seen that the XRD peaks of the Zn_2GeO_4 nanorods are broader than that of the micropheres and bulk Zn_2GeO_4 which indicates that the crystalline size of Zn_2GeO_4 nanorods is smaller than that of microspheres and bulk Zn_2GeO_4. This result is further confirmed by scanning electron microscopy analysis (Fig. 2). The crystal structure of Zn_2GeO_4 is shown in Fig. 1b. Zn_2GeO_4 is a binary compound oxide consisting of ZnO and GeO_2 with the space group *R*3 and has a phenacite structure with lattice constants of $a = b = 14.231$ Å and $c = 9.53$ Å. The coordination number of Zn, Ge, O atoms is 4, 4, 3, respectively.

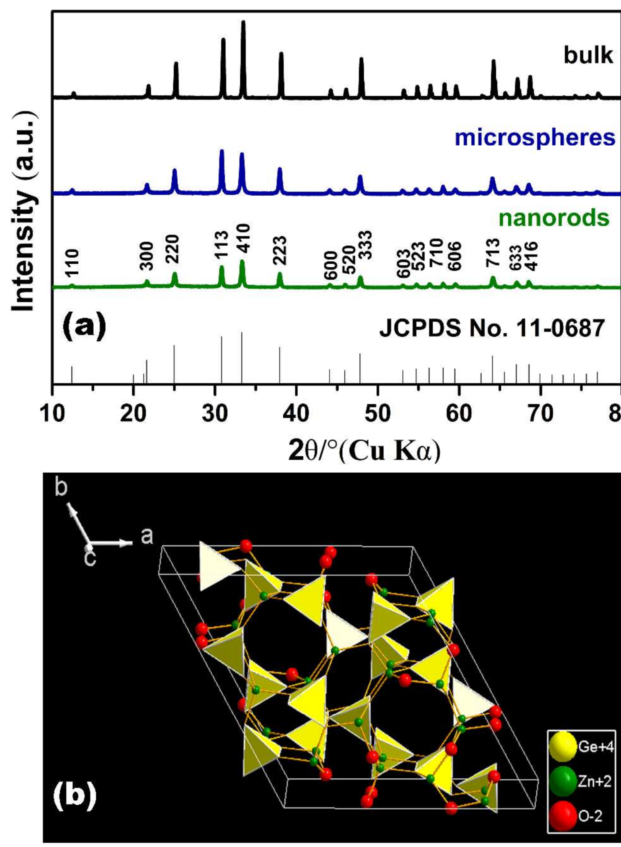

Fig. 1 (a) XRD pattern of Zn_2GeO_4. The standard data of Zn_2GeO_4 (JCPDS No. 11-0687) as reference;(b) crystal structure of Zn_2GeO_4 with a unit cell.

The morphology and microstructure of the as-prepared products were investigated by SEM, FESEM and TEM. Fig. 2a and b, we can clearly see that the asobtained Zn_2GeO_4 consists of nanorods with smooth surface and perfect prism structure. The length of these nanorods is approximately 100 ‑ 200 nm, and the diameter ranges from 10 to 20 nm. The sample prepared at 170 ºC for 10 min is composed of well-dispersed Zn_2GeO_4 microspheres with diameters ranging from 1–5 µm (Fig. 2c and d). The inset image in Fig.2c further shows that the single Zn_2GeO_4 microsphere is constructed of randomly packed nanorods which are about 20-50 nm in length and 10-20 nm in width. Fig.2e show TEM image of the rhombohedral Zn_2GeO_4 nanorods, and the corresponding HRTEM results. The HRTEM image (Fig. 2f) shows well-resolved lattice fringes with an interplanar distance of 0.27 nm corresponding to the (410) d spacing of the rhombohedral Zn_2GeO_4 structure[31].

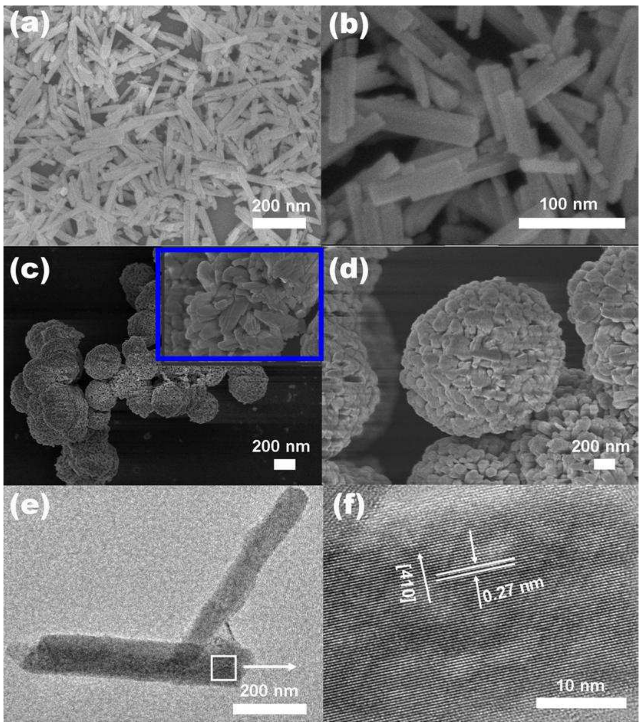

Fig. 2 SEM images of as-synthesized Zn_2GeO_4 nanorods (a, b) and SEM images of as-synthesized Zn_2GeO_4 microspheres (c,d). TEM image of the nanorods crystal lattice (e) and HRTEM images of the nanorods(f).

Influencing factors. In order to reveal factors influencing the formation of nanorods of Zn_2GeO_4, some controlled experiments have been carefully performed by changing one reaction parameter (reaction temperature, the urea, and reaction time) while the other reaction conditions are kept constant.

The effect of reaction temperature. It should be noted that the samples prepared at this temperature were not aligned well and bound tightly. When the temperature was controlled at 100 ºC, the product was comprised of nanoparticles agglomeration were represented (Fig. 3a). However, the corresponding XRD pattern shown in Fig. S1a indicated that the product was a mixed phase of rhombohedral phase Zn_2GeO_4 (JCPDS file Card No. 11-0687), hexagonal $Zn(OH)_2$ (JCPDS file Card No. 72-2032) and hexagonal GeO_2 (JCPDS file Card No. 830548)[10].It is found that the variation of reaction temperature greatly changes the product morphology and phase. When the reaction was carried out at 140 ºC for 10 min, keeping other experimental parameters constant, hexagonal prism Zn_2GeO_4 nanorods were produced (Fig. 3c and S1c). To further obtain the detailed crystal structure of the prismatic Zn_2GeO_4 nanorods and nanofibers, HRTEM observations were obtained. Figures 3d show typical TEM images of the hexagonal Zn_2GeO_4 nanorods, and the corresponding HRTEM results. It is clearly observed that the lattice fringes are parallel to the growth direction of the rod. In Figure 3d, the lattice fringe of the (300) plane with an interplanar spacing of 0.41 nm is observed parallel to the nanorod direction. According to the above structure information, we can conclude that the hexagonal Zn_2GeO_4 nanorods grew along the direction of the c-axis of the rhombohedral phenacite-type structure.

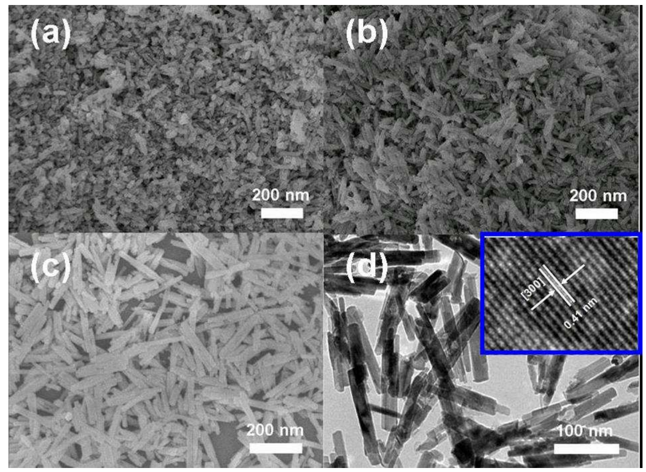

Fig. 3 SEM images of the products at different reaction temperatures: (a) 100 ºC, (b) 120 ºC and 140 ºC. TEM images and HRTEM image of the as-prepared Zn_2GeO_4 nanorod.

The morphology and microstructure of the as-prepared microspheres were investigated by SEM, FESEM and TEM. Fig. 4a shows that the Zn_2GeO_4 is composed of irregular particles at 100 ºC for 10 min. The samples obtained by the microwave-assisted process at 120 and 140 ºC for 10 min consist of some agglomerated Zn_2GeO_4 nanorods (Fig. 4b and c).

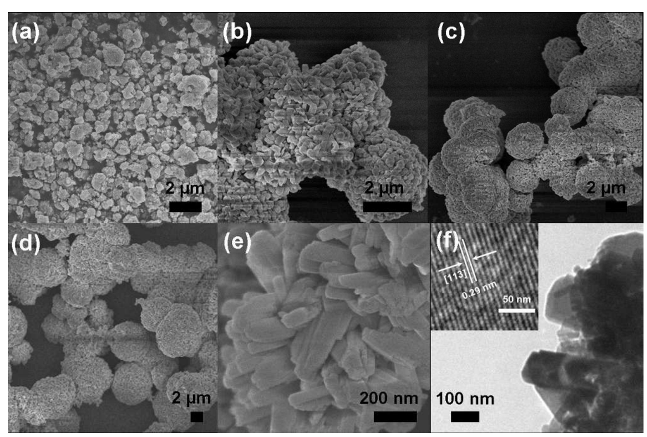

Fig.4 SEM images of the products at different reaction temperatures: (a) 100 ºC, (b) 120 ºC, (c) 140 ºC, (d) 170 ºC, (e) FESEM image further shows that the single Zn_2GeO_4 microsphere is constructed of randomly packed nanosheets, (f) TEM and HRTEM images of the individual Zn_2GeO_4 microspheres.

The sample prepared at 170 ºC for 10 min is composed of well-dispersed Zn_2GeO_4 microspheres with diameters ranging from 1–5 µm (Fig. 4d). The FESEM image in Fig. 4e further shows that the single Zn_2GeO_4 microsphere is constructed of randomly packed nanorods which are about 20-50 nm in length and 10-20 nm in width.This result is in agreement with that of XRD analyses (Fig. S2). Some of microspheres can be found in Fig. 4f, which were further were investigated by TEM. Fig. 4f shows a typical high-resolution transmission electron microscopy image of Zn_2GeO_4 nanorods. Well-resolved lattice fringes are clearly visible, with an interplanar d spacing of 0.29 nm corresponding to the (113) lattice planes of the rhombohedral Zn_2GeO_4 structure, indicating good crystallization of the prepared Zn_2GeO_4 microspheres.

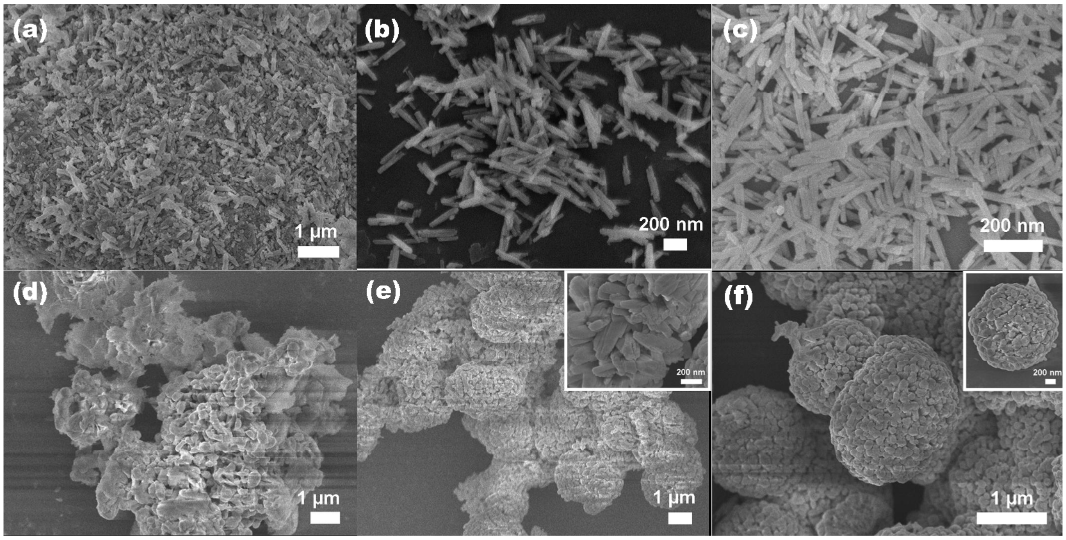

Fig.5 SEM images of the nanorods at 140 ºC with different reaction time: (a) 1 min, (b) 5 min and (c) 10 min; SEM images of the microspheres at 170 ºC with different reaction time: (d) 1 min, (e) 5 min and (f) 10 min.

The effect of reaction time and the formation mechanism. To understand the formation of the Zn_2GeO_4 nanorods, we carried out time-dependent shape evolution experiments during which samples were collected after different periods of microwave-assisted treatment. At an early stage 1 min, the supersaturated solution leads to the nucleation of Zn_2GeO_4 On the basis of the experimental results, the formation mechanism for the Zn_2GeO_4 nanorods is speculated to be as follows: (1) In the synthetic process, GeO_2 is hydrolyzed to form GeO_3^{2-}; (2) When the concentrations of Zn^{2+} and GeO_3^{2-} reach the supersaturation degree of Zn_2GeO_4, small Zn_2GeO_4 nuclei formaccording to the following equation: $2Zn^{2+} + GeO_3^{2-} + 2OH^- = Zn_2GeO_4 + H_2O$. (3) These nuclei further growalong the *c*-axis to produce Zn_2GeO_4 nanorods.

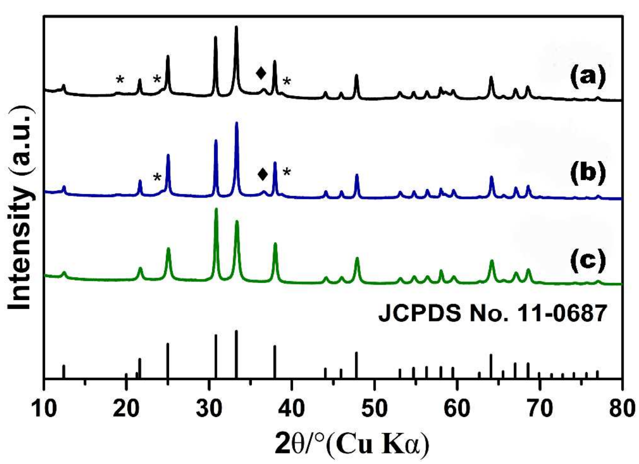

Fig.6 XRD pattern of Zn_2GeO_4 nanorods 140 ºC with different reaction time: (a) 1 min, (b) 5 min and (c) 10 min,∗:$Zn(OH)_2$;♦:GeO_2.

and tiny Zn_2GeO_4 particles are formed from the solution (Fig. 5a). The corresponding XRD pattern shown in Fig. 6a, indicated that the sample was a mixed phase with rhombohedral Zn_2GeO_4, hexagonal $Zn(OH)_2$ and GeO_2. The sample collected 5 min later (Fig. 5b and 6b) shows approximately nanorods with length of 100-200 nm. As the reaction proceeded (Fig. 5c and 6c), the smooth nanorods with perfect prism structure developed. In order to monitor the morphological evolution and reveal the possible growth mechanism of the Zn_2GeO_4 microspheres, a series of time-dependent experiments were carefully carried out to gain an insight into the formation process. When the reaction time was controlled at 1 min, the SEM image indicated that the product was comprised of nanoparticles and nanosheets (Fig. 5d). Prolonging the reaction time to 5 min, the yield of Zn_2GeO_4 microspheres gradually increased which was comprised of nanosheet-assembled hollow spheres (Fig. 5e). Further prolonging to 10 min, well-aligned Zn_2GeO_4 microspheres were harvested (Fig. 5f). It can be concluded that with increasing reaction time, $Zn(OH)_2$ and GeO_2 gradually disappear and more and more Zn_2GeO_4 microspheres are formed. The corresponding XRD pattern shown in Fig. S3, From the conditional experiments such as variation of reaction time and temperature, one can find that the products prepared at low reaction temperature or with a short reaction time usually contain the impurities phase of hexagonal $Zn(OH)_2$ and GeO_2. With increasing reaction temperature and time, these impurities gradually disappear.

From the time-dependent experiments, it can be concluded that the possible reactions involved in the reaction process could be summarized by eqn (1)–(4).

$$CO(NH_2)_2 + H_2O \rightarrow CO_2 + 2NH_3 \quad (1)$$

$$NH_3 + H_2O \leftrightarrow NH_3{\cdot}H_2O \leftrightarrow NH_4^{\ +} + OH^- \quad (2)$$

$$GeO_2 + OH^- \leftrightarrow HGeO_3^- \quad (3)$$

$$2Zn^{2+} + HGeO_3^- + 3OH^- \leftrightarrow Zn_2GeO_4 + 2H_2O \quad (4)$$

The whole evolution process is illustrated in the scheme of Fig. 7. The photocatalytic performance of the as-prepared Zn_2GeO_4 nanorods was evaluated by a water splitting reaction in the presence of methanol under UV-light irradiation. For comparison, the photocatalytic activities of the P25 TiO_2 and the Zn_2GeO_4 microspheres were also determined. The hydrogen evolution amounts as a function of reaction time are shown in Fig. 8a. For all samples, the hydrogen production over each catalyst increases proportionally with the reaction time, but all the Zn_2GeO_4 samples show higher activity than the P25 TiO_2.

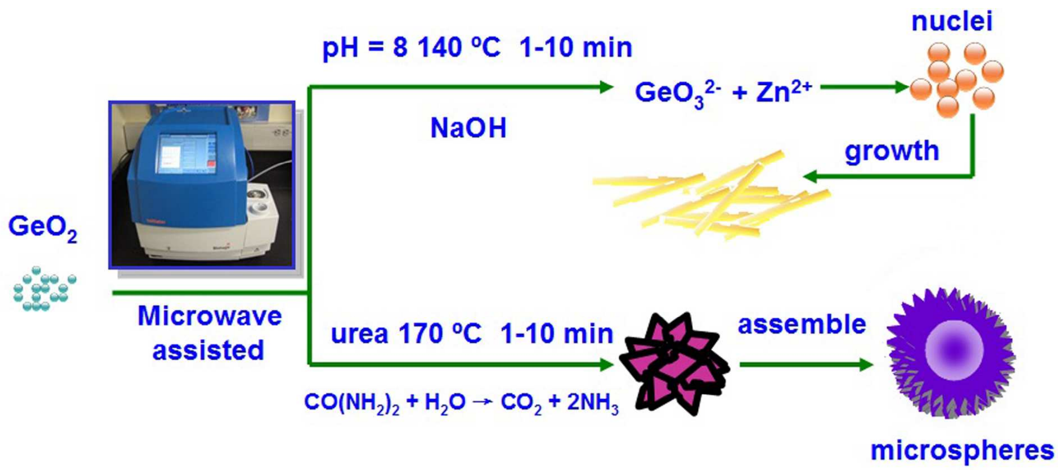

Fig.7 Scheme 1 The scheme for synthesizing Zn_2GeO_4 hexagonal prism Zn_2GeO_4 nanorods and hierarchical microspheres

The nanorods and microspheres of photocatalysts Zn_2GeO_4 were synthesized by a microwave-assisted solution method and investigated for photocatalytic hydrogen generation from water-methanol solution.The controlled blank reaction in the absence of any catalyst showed there was no H_2 formation. The photocatalytic activities were also compared with those of the P25 TiO_2 and bulk Zn_2GeO_4 particles. As shown in Fig. 8b, it is found that the nanostructure Zn_2GeO_4 efficiently improves the photocatalytic activity which exhibits 6.24 mmol g^{-1} h^{-1} hydrogen evolution, which is more than 3 times higher than bulks of Zn_2GeO_4 with calcination. The nanostructured samples are markedly superior in activity to the bulk sample prepared by general solid-state reaction routes. The photocatalytic activity on Zn_2GeO_4 (microspheres) is also shown for comparison. It is very clear that the photocatalytic activity of microspheres synthesized *via* microwave-assisted solution is much lower than that of nanorods. For comparison, the photocatalytic performances of Zn_2GeO_4 and a commercially available TiO_2 (P25) were also tested, which showed a superior photocatalytic H_2 evolution activity to the benchmark P25 TiO_2. Wang and his co-workers synthesized hexagonal nanorods and nanofibers via hydrothermal method, and the photocatalytic activities were also compared with those of the P25 TiO_2 and bulk Zn_2GeO_4 particles[1].

the Zn_2GeO_4 nanorods show the highestactivity, and the hydrogen evolution rate is decreased in the order nanorods > microspheres > bulks. Which is nearly 2 times higher than that on the microspheres. The results show that the rod structure of hexagonal Zn_2GeO_4 nanorods with dominant (110) facets greatly improves photocatalytic hydrogen-evolving properties of the 1-D nanostructures.

The DFT calculation of Zn_2GeO_4 showed that the top of the valence band is composed of the O 2p orbital, while the bottom of the conduction band is composed of the Ge 4p orbital with a small contribution of the Zn 4*s*4*p* orbitals. Such a conduction band is highly dispersive, and therefore leads to large mobility of photoexcited electrons.

In Fig. 8a, the Zn_2GeO_4 nanorods shows a stable H_2 evolution rate of 6.24 mmol g^{-1} h^{-1} under UV light. The discussion about different morphologie of samples sprepared at different synthetic routes of Zn_2GeO_4 was listed in Table S1. Wang *et al*. reported a highly regular, crystal orientation ordered and tight-binding Zn_2GeO_4 bundle, which was assembled from hexagonal nanoprism monomers *via* a triethanolamine (TEA)-induced self-assembly process under mild solvothermal conditions. The H_2-producing rate on the Zn_2GeO_4 bundles is surprisingly up to (4.9 mmol g^{-1} h^{-1})[1]. Liang and his co-workers developed a simple hydrothermal synthesis technique without any organic additives, and unexpectedly obtain hexagonal Zn_2GeO_4 nanorods and nanofibers with a high aspect ratio. The hexagonal Zn_2GeO_4 nanorods showed the highest rate of H_2 evolution[12], and the evolution rate of hydrogen gas was 6.0 mmol g^{-1} h^{-1}. Hierarchical Zn_2GeO_4 hollow spheres were fabricated *via* a synergistic self-assembly route by Xu and his co-workers[11]. The H_2-producing rate on the Zn_2GeO_4 hollow spheres was surprisingly up to (6.23 mmol g^{-1} h^{-1}). We reported the synthesis of photocatalytic materials with different morphology *via* microwave-assisted mthod. The microwave-assisted synthetic material was used as an efficient photocatalytic material for H_2 evolution reaction. This work is expected to open up new synthetic avenues towards the preparation of other advanced inorganic nanomaterials with unique structures/composition for various applications, such as photocatalysis and gas sensing.

Cite this: DOI: 10.1039/c0xx00000x
www.rsc.org/xxxxxx

ARTICLE TYPE

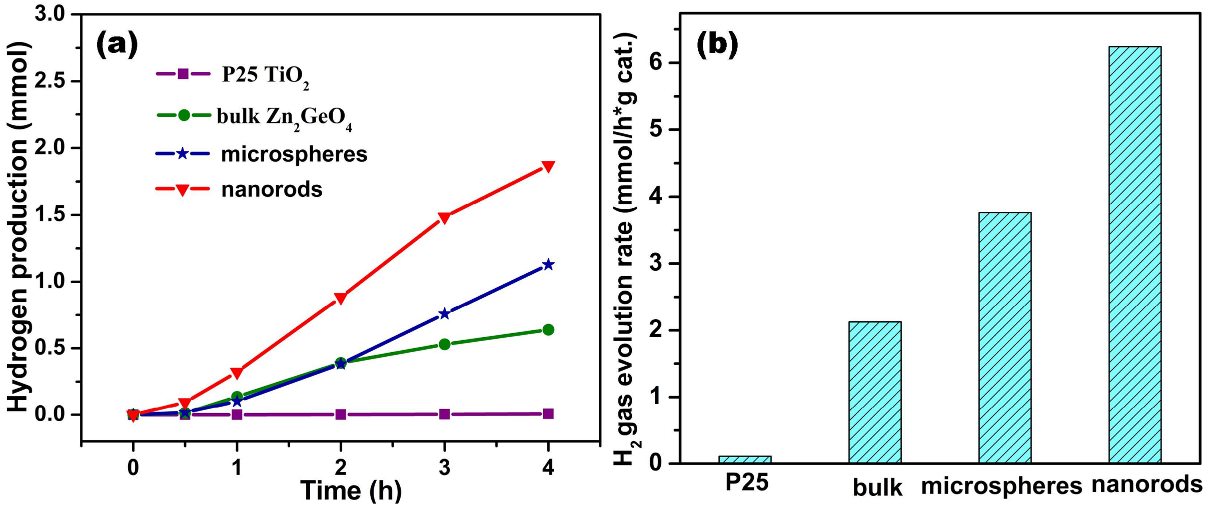

Fig.8 (a) Photocatalytic hydrogen evolution and (b) hydrogen evolution rate from an aqueous methanol solution over various photocatalysts under exposure to UV light. Catalyst amount, 0.075 g; H_2O volume, 75 mL; CH_3OH volume, 5 mL.

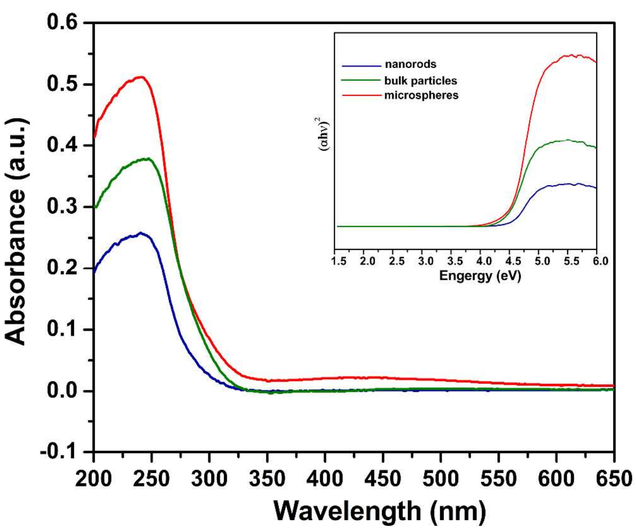

Fig.9 UV−visible light diffuse reflectance spectroscopy (UV-vis) spectra of the bulk Zn_2GeO_4 particles, hexagonal Zn_2GeO_4 nanorods, and Zn_2GeO_4 microspheres. Inset shows the optical band gap energy (Eg) of the corresponding sample.

The optical absorption properties of several Zn_2GeO_4 samples were investigated. The diffuse absorption spectra in Fig. 9 show that the bulk particles, nanorods, and microspheres, have a bandgap of ca. 4.2, 4.25 and 4.45 eV, respectively, corresponding to an optical absorption edge of about 295, 291, and 278 nm. The light absorption edges of nanostructured Zn_2GeO_4 samples exhibit a certain extent of blue shift in comparison with those of bulk Zn_2GeO_4 particles, which can be explained by size effects[32]. However, there is no signifcant difference in the absorption edges of the nanostructured Zn_2GeO_4 samples. So the difference in the bandgap is not the main reason leading to the discrepancy in their photocatalytic activity. In addition, the optical absorption intensities are decreased in the order microspheres > bulk > nanorods, while the photocatalytic activities are decreased in the order nanorods > microspheres > bulk (Fig. 8b). Apparently, the difference in the photo-absorption is also not the main factor leading to the difference in the photocatalytic activity.

Conclusions

In summary, we present a simple one-pot template-free microwave-assisted route for the synthesis of Zn_2GeO_4 nanorods and microspheres. The investigation on the evolution formation reveals that the microwave irradiation time played an important role in the formation of the Zn_2GeO_4 microspheres. High reaction temperature and long reaction time facilitate the formation of pure phase Zn_2GeO_4 product. For the photocatalytic activities of Zn_2GeO_4 samples, the Zn_2GeO_4 nanorods show the highestactivity, and the hydrogen evolution rate is decreased in the order nanorods > microspheres > bulks. Moreover, The photocatalytic investigations show that well-formed 1-D Zn_2GeO_4 nanorods exhibit excellent photocatalytic activities in the photocatalytic decomposition of a water−methanol solution to hydrogen under UV irradiation. Compared to existing solution-phase synthetic methods using hydrothermal reactions, this paper provides a facile, rapid, low-cost pathway to novel Zn_2GeO_4 nanoarchitectures.

Acknowledgements

This work was supported by the National Natural Science Foundation of China (No.21271082).

Notes and references

[a] *State Key Laboratory of Inorganic Synthesis and Preparative Chemistry, College of Chemistry, Jilin University, Changchun 130012, PR China Tel/Fax: +86-431-85168316.*
E-mail address: liuxy@ jlu.edu.cn (X.Y.Liu).
[b] *Address, Address, Town, Country. Fax: XX XXXX XXXX; Tel: XX XXXX XXXX; E-mail: xxxx@aaa.bbb.ccc*

† Electronic Supplementary Information (ESI) available: [details of any supplementary information available should be included here]. See DOI: 10.1039/b000000x/

‡ Footnotes should appear here. These might include comments relevant to but not central to the matter under discussion, limited experimental and spectral data, and crystallographic data.

1 A. Name, B. Name and C. Name, *Journal Title*, 2000, **35**, 3523; A. Name, B. Name and C. Name, *Journal Title*, 2000, **35**, 3523.

1. J. Liang, J. Xu, Q. Gu, Y. Zhou, C. Huang, H. Lin and X. Wang, *Journal of Materials Chemistry A*, 2013, **1**, 7798.
2. A. J. B. a. M. A. Fox, *Acc. Chem. Res.,* 1995, **28**.
3. S. Yan, J. Wang and Z. Zou, *Dalton transactions,* 2013, **42**, 12975
4. S. Yan, J. Wang, H. Gao, N. Wang, H. Yu, Z. Li, Y. Zhou and Z. Zou, *Advanced Functional Materials*, 2013, **23**, 1839
5. J. Wang, C. Yan, S. Magdassi and P. S. Lee, *ACS applied materials & interfaces*, 2013, **5**, 6793
6. L. Z. Pei, S. Wang, Y. X. Jiang, Y. K. Xie, Y. Li and Y. H. Guo, *CrystEngComm*, 2013, **15**, 7815.
7. M.-Y. Tsai, S.-H. Huang and T.-P. Perng, *Journal of Luminescence*, 2013, **136**, 322
8. L. Liu, X. Zhao, H. Sun, C. Jia and W. Fan, *ACS applied materials & interfaces*, 2013, **5**, 6893
9. J. Liu, G. Zhang, J. C. Yu and Y. Guo, *Dalton transactions*, 2013, **42**, 5092.
10. J. Liu and G. Zhang, *CrystEngComm*, 2013, **15**, 382.
11. J. Liang, J. Xu, J. Long, Z. Zhang and X. Wang, *Journal of Materials Chemistry A*, 2013, **1**, 10622.
12. J. Liang, Y. Cao, H. Lin, Z. Zhang, C. Huang and X. Wang, *Inorganic Chemistry*, 2013, **52**, 6916.
13. N. Zhang, S. Ouyang, T. Kako and J. Ye, *Chemical communications*, 2012, **48**, 9894.
14. S. Takeshita, J. Honda, T. Isobe, T. Sawayama and S. Niikura, *Journal of Solid State Chemistry*, 2012, **189**, 112.
15. N. Zhang, S. Ouyang, P. Li, Y. Zhang, G. Xi, T. Kako and J. Ye, *Chemical communications*, 2011, **47**, 2041.
16. J. K. Feng, M. O. Lai and L. Lu, *Electrochemistry Communications*, 2011, **13**, 287.
17. C. Yan, N. Singh and P. S. Lee, *Applied Physics Letters*, 2010, **96**, 053108.
18. J. D. Huang, K.; Hou, Y.; Wang, X. X.; Fu, X. Z., *ChemSusChem*, 2008, **1**, 1011.
19. C. Y. L. Yan, P. S., *J. Phys. Chem. C*, 2009, **113**, 14135.
20. G. Tan, L. Zhang, H. Ren, S. Wei, J. Huang and A. Xia, *ACS applied materials & interfaces*, 2013, **5**, 5186.
21. L. C. Mostafa Baghbanzadeh, P. Davide Cozzoli, and and C. O. Kappe, *Angew. Chem. Int. Ed.*, 2011, **50**, 11312.
22. Q. H. Z. X.X. Zhu, Y.G. Li, H.Z. Wang, *J. Mater. Chem.*, 2010, **20**, 1766.
23. W. C. C. a. K. S. Y. G. A. Tompsett, *ChemPhysChem*, 2006, **7**, 296.
24. I. D. a. M. N. I. Bilecka, *Chem. Commun*, 2008, 886.
25. S. Y. L. S. H. Kim, G. R. Yi, D. J. Pine and S. M. Yang, *J. Am.Chem. Soc*, 2006, **128**, 10897.
26. T. a. Mulinari, F. a. La Porta, J. Andrés, M. Cilense, J. a. Varela and E. Longo, *CrystEngComm*, 2013, **15**, 7443.
27. X. Li, P. Sun, T. Yang, J. Zhao, Z. Wang, W. Wang, Y. Liu, G. Lu and Y. Du, *CrystEngComm*, 2013, **15**, 2949.
28. M. Sun, D. Li, W. Zhang, Z. Chen, H. Huang, W. Li, Y. He and X. Fu, *Journal of Solid State Chemistry*, 2012, **190**, 135.
29. F. Zou, X. Hu, Y. Sun, W. Luo, F. Xia, L. Qie, Y. Jiang and Y. Huang, *Chemistry*, 2013, **19**, 6027.
30. Y. Z. Q. Liu, J. H. Kou, X. Y. Chen, Z. P. Tian, J. Gao, S. C. Yan and Z. G. Zou, *J. Am. Chem. Soc.*, 2010, , **132**, 14385.
31. M. Shang, G. Li, D. Yang, X. Kang, C. Peng, Z. Cheng and J. Lin, *Dalton transactions*, 2011, **40**, 9379.
32. Y. D. Zhang, F.; Wu, J.; Liu, L.; Chen, M. Q.; Xie, Y, *J. Mol.Catal. A: Chem.*, 2009, **303**, 9.